ORGANIC CHEMISTRY

# Highly enantioselective carbene insertion into N–H bonds of aliphatic amines

Mao-Lin Li, Jin-Han Yu, Yi-Hao Li, Shou-Fei Zhu*, Qi-Lin Zhou*

Aliphatic amines strongly coordinate, and therefore easily inhibit, the activity of transition-metal catalysts, posing a marked challenge to nitrogen-hydrogen (N–H) insertion reactions. Here, we report highly enantioselective carbene insertion into N–H bonds of aliphatic amines using two catalysts in tandem: an achiral copper complex and chiral amino-thiourea. Coordination by a homoscorpionate ligand protects the copper center that activates the carbene precursor. The chiral amino-thiourea catalyst then promotes enantioselective proton transfer to generate the stereocenter of the insertion product. This reaction couples a wide variety of diazo esters and amines to produce chiral α-alkyl α–amino acid derivatives.

Chiral amines are ubiquitous in natural products, pharmaceuticals, and agrochemicals. Approximately 43% of the top 200 prescription medicines in 2016 contain an aliphatic amine moiety (Fig. 1A) (*1*, *2*). The development of highly enantioselective transition-metal–catalyzed reactions that form C–N bonds is thus of long-standing interest in synthetic chemistry (*3*–*5*). Transition-metal–catalyzed carbenoid insertion into N–H bonds has proven a straightforward method in this respect, benefitting from mild reaction conditions, good functional group tolerance, and readily available reactants (*6*, *7*). Recently, chiral transition-metal catalysts have been successfully applied to enantioselective N–H insertion reactions in the synthesis of natural or unnatural chiral α–amino acid derivatives (*8*, *9*). However, these reactions have been restricted to aromatic amines (*10*–*15*) or amides (*16*–*18*) (Fig. 1B). Aliphatic amines are comparatively stronger Lewis bases and thus poison the metal catalysts by strong coordination, interfering with generation of the metal carbenoid (*19*, *20*). Moreover, excess aliphatic amines can displace the ylide from metal-ylide intermediates, leading to racemic product formation from the free ylide (Fig. 1C, upper). We envisioned that a combination of two catalysts (*21*, *22*) might address these challenges: An achiral transition-metal catalyst compatible with aliphatic amines would generate the ylide intermediate, and a separate chiral catalyst would then promote enantioselective proton transfer. After exploring various transition-metal catalysts and chiral H-bonding catalysts in the N–H insertion reaction of α-diazobutanoates with benzylamine (tables S1 to S5), we report here the success of this approach, pairing the homoscorpionate-coordinated copper complex Tp*Cu [Tp* is hydrotris(3,5-dimethylpyrazolyl) borate] (*23*–*25*) with a chiral amino-thiourea (CAT) bearing a pyrrolidine motif (*26*–*29*) (Fig. 1C, lower). The reaction provides efficient, highly enantioselective access to chiral α-alkyl α–amino acid derivatives bearing secondary and tertiary amino substituents, which are difficult to prepare by other methods.

Under the optimal reaction conditions, a broad range of aliphatic amines was then investigated for N–H insertion with 2-phenylpropan-2-yl α-diazobutyrate **2** (Fig. 2A). The benzylic primary amines underwent the N–H insertion reaction smoothly to afford the corresponding α-aminobutanoic acid derivatives (**3** to **9**) in high yields (81 to 95%) with high enantioselectivities [88 to 92% enantiomeric excess (ee)], though 2-phenethylamine and *n*-butylamine gave moderate enantioselectivities (**10** and **11**). Secondary amines were also suitable substrates for the reaction but required longer reaction times and excess diazo compounds for satisfactory outcomes. Piperidine derivatives generally exhibited high enantioselectivities, and the introduction of electron-withdrawing groups ($CO_2Me$ and CN) at the 4-position led to higher yields (71 and 86%, respectively) and better enantioselectivities (90 and 94% ee, respectively) (**12** to **14**). Morpholine, substituted piperazines, and thiomorpholine also underwent the N–H insertion and gave the desired products (**15** to **19**) in high yield with 87 to 97% ee. Fused heterocyclic amines also afforded N–H insertion products in satisfactory yields and enantioselectivities (**20** and **21**). However, azepane and *N*-methyl-1-phenylmethanamine gave lower enantioselectivities (73 and 77% ee, respectively, **22** and **23**). The N–H insertion reactions with chiral drugs, such as amoxapine, trimetazidine, and vortioxetine, proceeded smoothly to afford corresponding α-aminobutanoic acid derivatives (**24** to **26**) in high yields with good enantioselectivities (Fig. 2B). The scope with respect to the diazo reactant in the N–H insertion of morpholine was investigated next (Fig. 2C). Diazo esters with linear or branched α-alkyl chains afforded the desired products in good to high yields (66 to 99%) with excellent enantioselectivities (94 to 96% ee) (**27** to **31**). Various functional groups (alkenyl, ester, ether, amide) appended to the alkyl chain were tolerated, giving high yields (86 to 99%) and enantioselectivities (87 to 96% ee) (**32** to **38**). Furthermore, α-aryl diazoacetates also afforded the corresponding arylglycine derivatives (**39** to **44**) in high yields (>95%) with good enantioselectivities (72 to 89% ee).

To demonstrate the further synthetic utility of the N–H insertion reaction, several transformations of the insertion products were performed. The product (*R*)-**3** was reduced by $LiAlH_4$ to afford (*R*)-2-benzylamino-butanol [(*R*)-**45**], an intermediate for the synthesis of γ-secretase inhibitors (*30*) and PDK1 inhibitors (*31*) (Fig. 3A). The product **15**, which could be prepared at gram scale from N–H insertion of morpholine and diazo ester **2**, was hydrolyzed to acid **46**, an intermediate for the synthesis of hyperproliferative disorder (HPD) treatment agents (Fig. 3B) (*32*). The (*R*)-2-morpholinopropanoic acid (**47**), which is prepared by hydrolysis of the product **27**, is a key intermediate for the synthesis of the phosphatidylinositol 3-kinase δ (PI3Kδ) inhibitors (*33*), as well as DNA-dependent protein kinase (DNA-PK) inhibitors (*34*) (Fig. 3C).

To gain deeper insight into the mechanism of the N–H insertion reaction, we performed kinetic analyses by using in situ infrared (IR) spectroscopy. To accelerate the kinetics, the initial rates of the reaction were measured at various concentrations of the components at 40°C (figs. S1 to S5). The rate showed a first-order dependence on concentrations of Tp*Cu and diazo compound **2** (Fig. 4A), which indicates that the formation of metal carbenoid through Tp*Cu-catalyzed decomposition of diazo ester **2** is the likely rate-limiting step. The negative first-order dependence on CAT is consistent with a pre-equilibrium formation of a resting-state complex between the thiourea catalyst CAT and Tp*Cu, which would suppress the copper-catalyzed decomposition of the diazo ester. However, benzylamine, generally coordinating with the metal catalyst and suppressing the formation of metal carbenoid, showed a zero-order kinetic effect in the reaction, which suggests that the coordination of CAT to Tp*Cu is much stronger than that of benzylamine, and the inhibition by benzylamine can be ignored (fig. S6). We posit that the negative Tp* ligand renders the copper catalyst a softer Lewis acid that favors interaction with a soft base like sulfur. Further evidence for the stronger interaction between CAT and Tp*Cu includes observations

State Key Laboratory and Institute of Elemento-Organic Chemistry, College of Chemistry, Nankai University, Tianjin 300071, China.
*Corresponding author. Email: sfzhu@nankai.edu.cn (S.-F.Z.); qlzhou@nankai.edu.cn (Q.-L.Z.)

of the changes in nuclear magnetic resonance (NMR) and ultraviolet (UV)–visible spectra after adding CAT into a mixture of Tp*Cu and benzylamine (figs. S7 to S11). Taken together, the kinetic, NMR, and UV studies are consistent with the Tp*Cu•CAT complex, rather than the Tp*Cu•$BnNH_2$ complex, as the resting state of the catalyst in the reaction. Although the Tp*Cu•CAT complex is the main resting state of the copper, free Tp*Cu is still evident under the reaction conditions (fig. S10) and can react with the diazo compound.

Density functional theory (DFT) calculations indicated that the copper catalyst in the intermediate Cu-ylide could be recoordinated by thiourea to release a free ylide or its more stable tautomer free enol (Fig. 4B). Even without the added chiral catalyst, the proton transfer of these intermediates is still a very rapid process and can be mediated by trace water, enol intermediates, and even substrates themselves (*18*, *35*). The similar p$K_a$ values (where $K_a$ is the acid dissociation constant) (figs. S12 to S14 and table S8) of the Brønsted acidic site and protonated basic site of the thiourea promote concerted proton transfer, whereby the thiourea protonates the newly formed stereogenic center, and the amino group deprotonates the free enol. Computational modeling of the Tp*Cu•CAT complex using DFT revealed a minimum energy structure in which bonding of the Tp*Cu to the sulfur atom of the thiourea enhances Brønsted acidity (Fig. 4B).

The enantio-determining proton-transfer step was studied computationally by using DFT with the Tp*Cu•CAT complex as a catalyst. The structures corresponding to the lowest-energy transition states for the major and minor enantiomers of product are presented in Fig. 4C. The optimal transition state TSRaCu-I is only 2.8 kcal/mol higher in free energy than the free enol, implying extremely efficient proton-transfer catalysis. In accord with experimental observations, the calculated energy of transition state TSRaCu-I was 4.9 kcal/mol lower than that of the TSSaCu-I transition state leading to the unfavored (*S*)-product of N–H insertion. Besides the different hydrogen-bonding interactions in the transition states TSRaCu-I and TSSaCu-I, the S–Cu bond in TSRaCu-I is markedly shorter than that in TSSaCu-I. The shorter S–Cu bond indicates stronger coordination of copper by thiourea and likely higher Brønsted acidity of the thiourea catalyst, which would promote proton transfer to the substrate.

Several other tris(pyrazolyl)borate (Tp) ligands bearing different substituents on the pyrazol rings were also evaluated under the standard reaction conditions (Fig. 4D). Despite a large fluctuation in the yield, the in situ IR studies showed that all tested Tp ligands promoted high conversions and that the major by-product was 2-phenylpropan-2-yl but-2-enoate, resulting from the β-H migration of the metal carbenoid (figs. S15 to S19). Modifying the Tp ligands also influenced the enantioselectivity when the same chiral thiourea catalyst was used, indicating involvement of the copper catalyst in the enantio-determining step. By contrast, upon tuning the electronic properties of the arene ring of the chiral thiourea catalyst, the enantioselectivity decreased precipitously, whereas the yield remained almost unchanged (table S7). We again hypothesize that copper coordination enhances the Brønsted acidity of the thiourea catalyst while minimally influencing the distant site of enantioinduction (Fig. 4C).

On the basis of the aforementioned mechanistic studies, a catalytic cycle is proposed in Fig. 4E. The Tp*Cu•CAT complex serves as a resting state of the catalyst and dissociates to release Tp*Cu, which catalyzes transformation of the diazo ester into the metal carbenoid in the rate-determining step. Nucleophilic attack on the metal carbenoid by the aliphatic amine

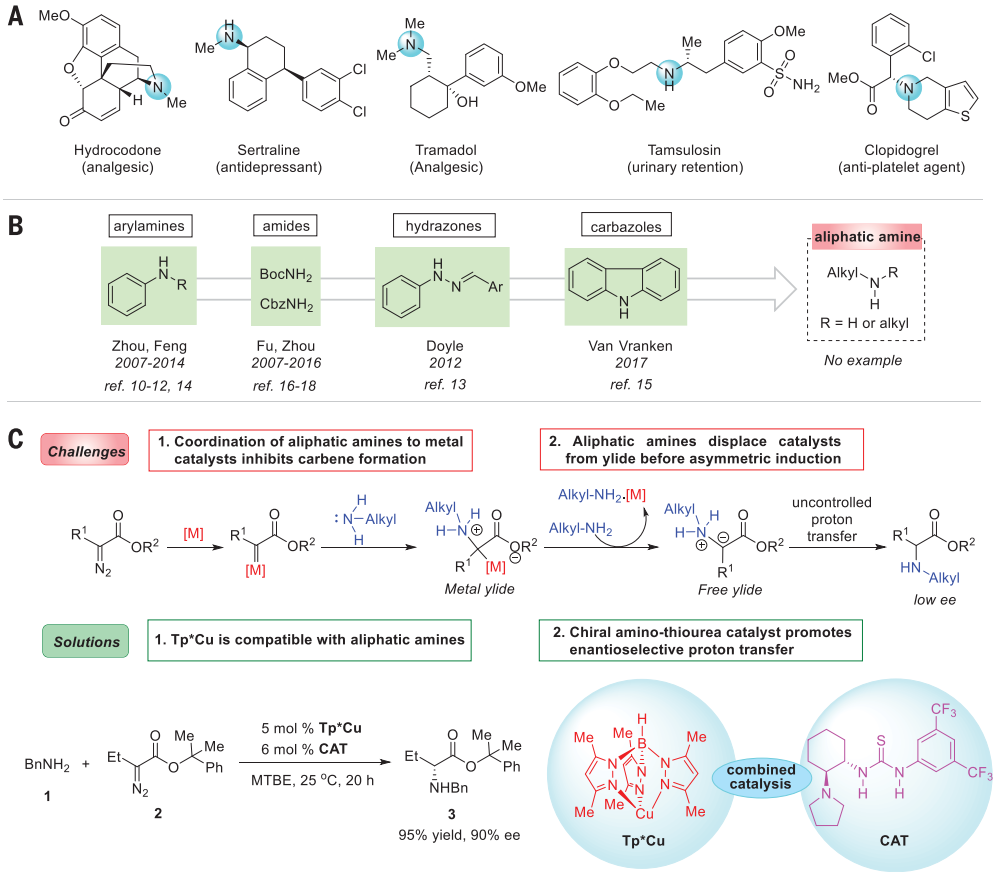


**Fig. 1. Strategy for enantiocontrol of N–H insertion reactions of aliphatic amines with carbenes.** (**A**) Representative drugs demonstrating the ubiquity of chiral aliphatic amines in bioactive molecules. (**B**) Amine sources reported for enantioselective N–H insertion reactions. (**C**) Enantioselective transition-metal–catalyzed N–H insertion reactions with aliphatic amines: challenges and solutions. Optimal reaction conditions: The reaction of **1** (0.2 mmol), **2** (0.22 mmol), Tp*Cu (5 mole %), and CAT (6 mol %) was carried out in 3 ml of methyl *tert*-butyl ether (MTBE) at 25°C for 20 hours. $BnNH_2$, benzylamine; $BocNH_2$, *tert*-butyl carbamate; $CbzNH_2$, benzyl carbamate; Me, methyl; Et, ethyl; Ph, phenyl; M, metal; ref., reference.

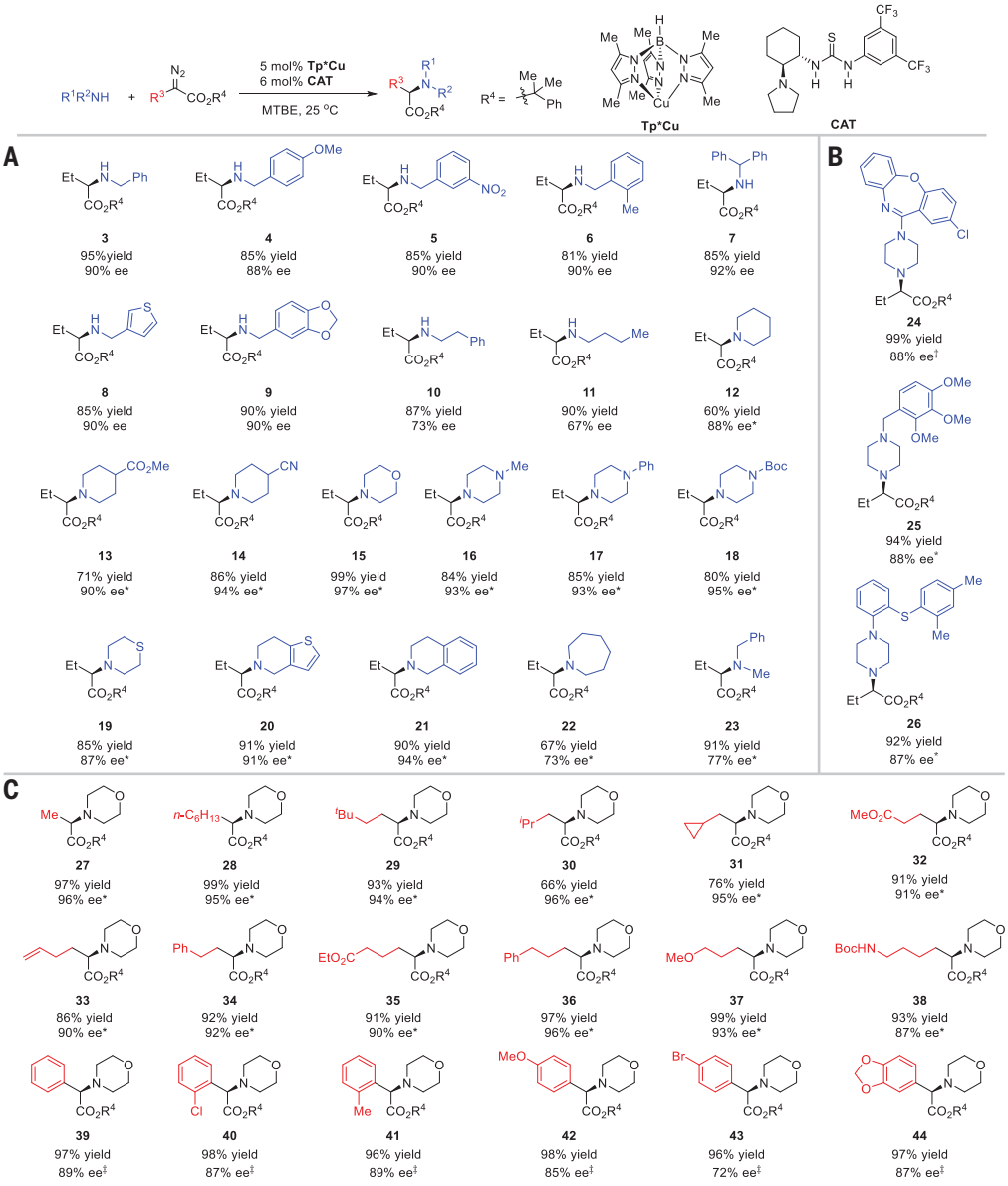


**Fig. 2. Scope of aliphatic amines and α-diazo esters in the enantioselective N–H insertion reaction.** Reaction conditions: amines (0.2 mmol), α-diazo esters (0.22 mmol), Tp*Cu (5 mol %), CAT (6 mol %), 3 ml MTBE, 25°C, 20 hours. Isolated yields are given. The ee values were determined by high-performance liquid chromatography. (**A**) Scope of aliphatic amines. (**B**) Application to enantioselective late-stage functionalization of pharmaceuticals. (**C**) Scope of α-diazo esters. *Diazo esters (0.3 mmol), 36 hours. †Diazo esters (0.3 mmol), MTBE:$CH_2Cl_2$ = 10:1, 36 hours. ‡Diazo esters (0.3 mmol), 40°C, 20 hours. $^t$Bu, *tert*-butyl; $^i$Pr, *iso*-propyl.

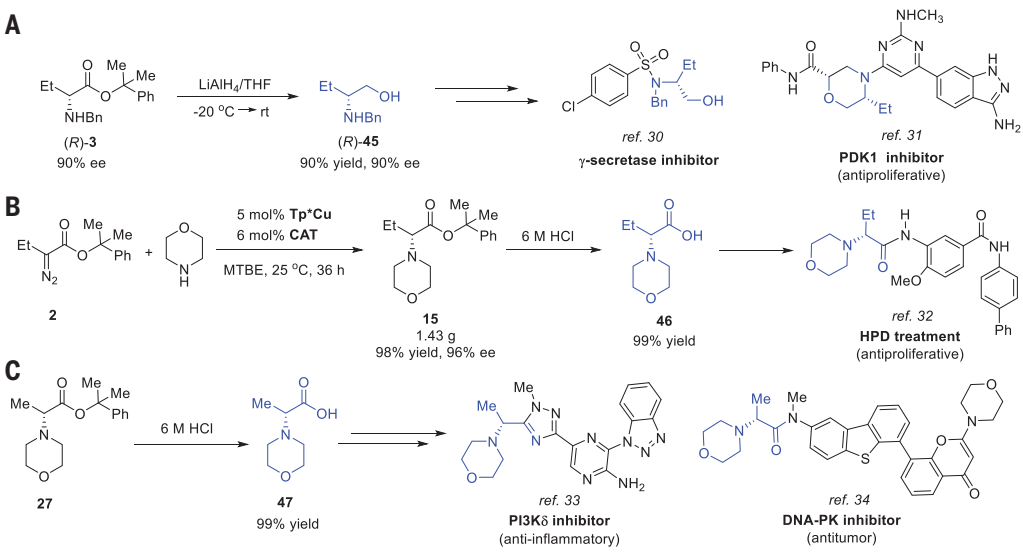


**Fig. 3. Synthetic transformations of the N–H insertion products.** (**A**) Transformation of **3** to (*R*)-2-benzylamino-butanol [(*R*)-**45**], a key intermediate for the synthesis of bioactive molecules. THF, tetrahydrofuran; rt, room temperature. (**B**) Formal synthesis of HPD treatment agents with the N–H insertion as key step. (**C**) Transformation of **27** to **47**, a key intermediate for the synthesis of bioactive molecules.

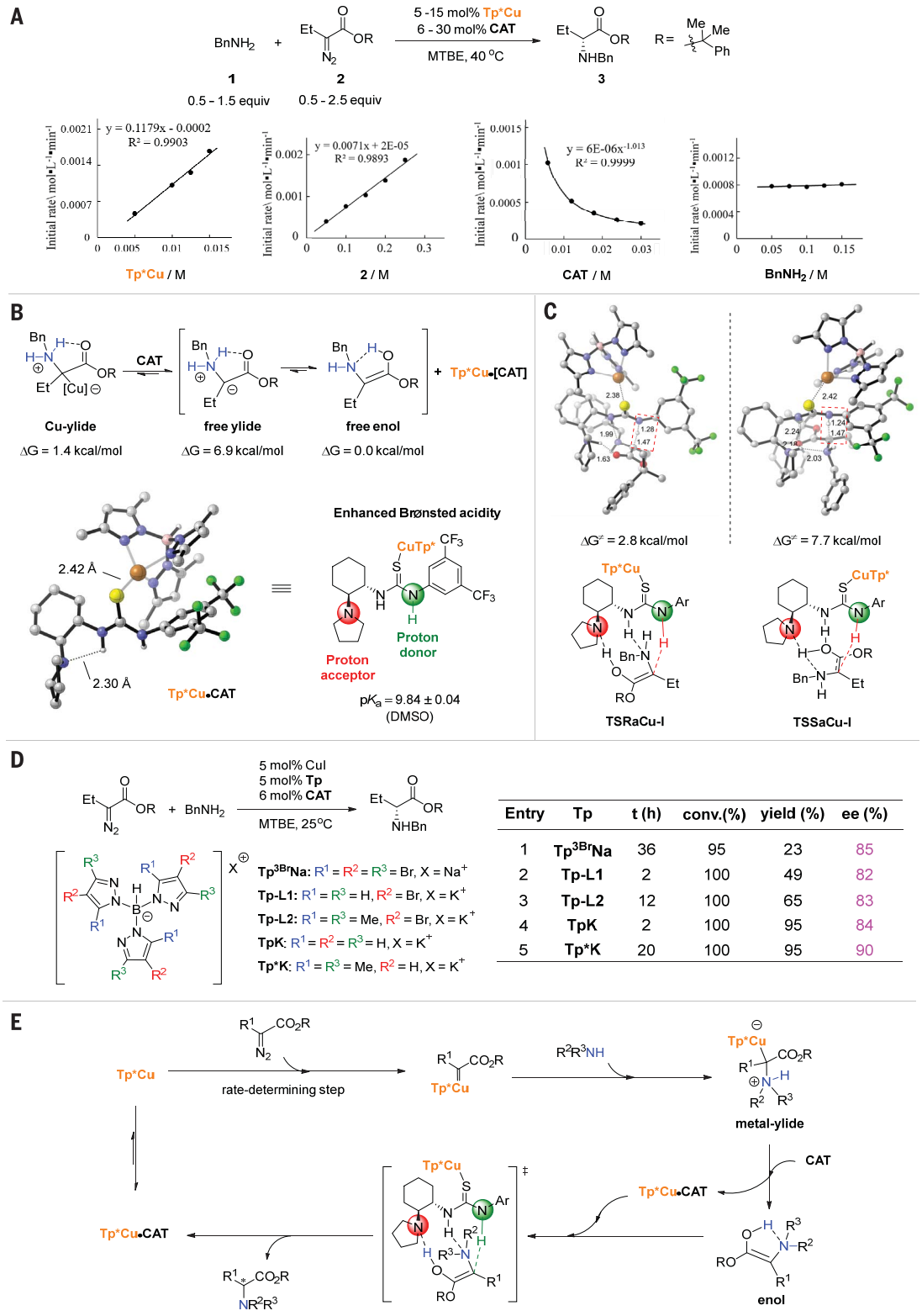


| Entry | Tp | t (h) | conv.(%) | yield (%) | ee (%) |
|---|---|---|---|---|---|
| 1 | $Tp^{3Br}Na$ | 36 | 95 | 23 | 85 |
| 2 | Tp-L1 | 2 | 100 | 49 | 82 |
| 3 | Tp-L2 | 12 | 100 | 65 | 83 |
| 4 | TpK | 2 | 100 | 95 | 84 |
| 5 | Tp*K | 20 | 100 | 95 | 90 |

**Fig. 4. Mechanistic studies.** (**A**) Kinetic profiles of Cu-catalyzed N–H insertion reaction of **2** and $BnNH_2$. (**B**) Calculated Gibbs free energy (ΔG) of Cu-ylide, free ylide, and free enol. Lowest-energy ground-state structure of the Tp*Cu•CAT complex. Structures of alternative higher-energy complexes are provided in fig. S20. (**C**) DFT-optimized lowest-energy transition structures for *R* and *S* products. Calculations were performed at the m062x-D3/def2tzvpp//m062x-D3/def2svp level. Structures of alternative higher-energy complexes are provided in figs. S21 to S25. (**D**) Influence of different Tp ligands. (**E**) Proposed catalytic cycle for the enantioselective carbene insertion into N–H bonds of aliphatic amines. conv., conversion; DMSO, dimethyl sulfoxide; equiv, equivalents.

generates a metal ylide. The catalyst CAT displaces the ylide from the metal-ylide intermediate to generate free enol and the Tp*Cu•CAT complex. The Tp*Cu•CAT complex then promotes proton transfer in the free enol through a push-pull mechanism: The amino moiety accepts a proton from the hydroxy group of the enol while the thiourea moiety donates a proton to the β-carbon of the enol.

The success of the overall transformation relies on the combined properties of the achiral copper catalyst and chiral organocatalyst. This study not only solves a long-standing challenge in enantioselective carbene insertion reactions

but also provides a potentially general strategy for transition-metal–catalyzed asymmetric transformations involving strongly coordinating substrates.

## REFERENCES AND NOTES


1. N. A. McGrath, M. Brichacek, J. T. Njardarson, *J. Chem. Educ.* **87**, 1348–1349 (2010).
2. These pharmaceutical posters are freely accessible to anyone as PDF files at https://njardarson.lab.arizona.edu.
3. T. C. Nugent, *Chiral Amine Synthesis: Methods, Developments and Applications* (Wiley VCH, 2010).
4. Y. Yang, S.-L. Shi, D. Niu, P. Liu, S. L. Buchwald, *Science* **349**, 62–66 (2015).
5. S.-L. Shi, Z. L. Wong, S. L. Buchwald, *Nature* **532**, 353–356 (2016).
6. M. P. Doyle, M. A. McKervey, T. Ye, *Modern Catalytic Methods for Organic Synthesis with Diazo Compounds* (Wiley, 1998).
7. A. Ford *et al*., *Chem. Rev.* **115**, 9981–10080 (2015).
8. S.-F. Zhu, Q.-L. Zhou, *Acc. Chem. Res.* **45**, 1365–1377 (2012).
9. D. Gillingham, N. Fei, *Chem. Soc. Rev.* **42**, 4918–4931 (2013).
10. B. Liu, S.-F. Zhu, W. Zhang, C. Chen, Q.-L. Zhou, *J. Am. Chem. Soc.* **129**, 5834–5835 (2007).
11. Z. Hou *et al*., *Angew. Chem. Int. Ed.* **49**, 4763–4766 (2010).
12. S.-F. Zhu, B. Xu, G.-P. Wang, Q.-L. Zhou, *J. Am. Chem. Soc.* **134**, 436–442 (2012).
13. X. Xu, P. Y. Zavalij, M. P. Doyle, *Angew. Chem. Int. Ed.* **51**, 9829–9833 (2012).
14. Y. Zhu *et al*., *Angew. Chem. Int. Ed.* **53**, 1636–1640 (2014).
15. V. Arredondo, S. C. Hiew, E. S. Gutman, I. D. U. A. Premachandra, D. L. Van Vranken, *Angew. Chem. Int. Ed.* **56**, 4156–4159 (2017).
16. E. C. Lee, G. C. Fu, *J. Am. Chem. Soc.* **129**, 12066–12067 (2007).
17. B. Xu, S.-F. Zhu, X.-L. Xie, J.-J. Shen, Q.-L. Zhou, *Angew. Chem. Int. Ed.* **50**, 11483–11486 (2011).
18. Y.-Y. Ren, S.-F. Zhu, Q.-L. Zhou, *Org. Biomol. Chem.* **16**, 3087–3094 (2018).
19. S. R. Hansen, J. E. Spangler, J. H. Hansen, H. M. L. Davies, *Org. Lett.* **14**, 4626–4629 (2012).
20. I. D. Jurberg, H. M. L. Davies, *Chem. Sci.* **9**, 5112–5118 (2018).
21. A. E. Allen, D. W. C. Macmillan, *Chem. Sci.* **2012**, 633–658 (2012).
22. D.-F. Chen, Z.-Y. Han, X.-L. Zhou, L.-Z. Gong, *Acc. Chem. Res.* **47**, 2365–2377 (2014).
23. S. E. Bromberg *et al*., *Science* **278**, 260–263 (1997).
24. S. Trofimenko, *Scorpionates: Polypyrazolylborate Ligands and Their Coordination Chemistry* (Imperial College Press, 1999).
25. M. E. Morilla *et al*., *Chem. Commun.* **2002**, 2998–2999 (2002).
26. M. S. Sigman, E. N. Jacobsen, *J. Am. Chem. Soc.* **120**, 4901–4902 (1998).
27. T. Okino, Y. Hoashi, Y. Takemoto, *J. Am. Chem. Soc.* **125**, 12672–12673 (2003).
28. S.-Z. Nie *et al*., *Tetrahedron Asymmetry* **21**, 2055–2059 (2010).
29. A. G. Doyle, E. N. Jacobsen, *Chem. Rev.* **107**, 5713–5743 (2007).
30. M. Neitzel, J. Marugg, WO patent 2005090296 (2005).
31. J. R. Medina *et al*., *J. Med. Chem.* **54**, 1871–1895 (2011).
32. K. Thede, W. J. Scott, E. Bender, S. Golz, A. Haegebarth, P. Lienau, F. Puehler, D. Basting, D. Schneider, M. Moewes, WO patent 2014147182 (2014).
33. I. Terstiege *et al*., *Bioorg. Med. Chem. Lett.* **27**, 679–687 (2017).
34. M. Frigerio, M. G. Hummersone, K. A. Menear, M. R. V. Finlay, E. J. Griffen, L. L. Ruston, J. J. Morris, A. K. T. Ting, B. T. Golding, R. J. Griffin, I. R. Hardcastle, S. Rodriguez-Aristegui, WO patent 2010136778 (2010).
35. Y. Liang, H. Zhou, Z.-X. Yu, *J. Am. Chem. Soc.* **131**, 17783–17785 (2009).


## ACKNOWLEDGMENTS


We thank X.-S. Xue for discussions of the DFT calculations and M. P. Doyle for comments and suggestions on the preparation of the manuscript. **Funding:** We thank the National Natural Science Foundation of China (21625204, 21790332, 21532003), the "111" project (B06005) of the Ministry of Education of China, and the National Program for Special Support of Eminent Professionals for financial support. **Author contributions:** Q.-L.Z. and S.-F.Z. conceived the study; M.-L.L., S.-F.Z., and Q.-L.Z. designed the experiments and analyzed the data; M.-L.L. performed the reactions and the mechanistic and DFT studies; J.-H.Y. and Y.-H.L. made some of the diazo substrates; and M.-L.L., S.-F.Z. and Q.-L.Z. wrote the manuscript. **Competing interests:** The authors declare no competing interests. **Data and materials availability:** Additional optimization and mechanistic data are provided in the supplementary materials.


## SUPPLEMENTARY MATERIALS

science.sciencemag.org/content/366/6468/990/suppl/DC1
Materials and Methods
Supplementary Text
Figs. S1 to S25
Tables S1 to S9
Spectral Data
Calculation Data
References (*36*–*69*)


20 February 2019; accepted 17 September 2019
10.1126/science.aaw9939

Science

# Highly enantioselective carbene insertion into N–H bonds of aliphatic amines

Mao-Lin Li, Jin-Han Yu, Yi-Hao Li, Shou-Fei Zhu and Qi-Lin Zhou

*Science* **366** (6468), 990-994.
DOI: 10.1126/science.aaw9939

**A tag team approach to forming C–N bonds**

Many pharmaceutical compounds contain carbon-nitrogen (C–N) bonds in just one of two mirror-image orientations. Forging these bonds with electron-rich nitrogen reactants is challenging because the nitrogen groups can coordinate with, and thus interfere with, the catalyst. Li *et al.* report a cooperative approach to overcoming this obstacle (see the Perspective by Ovian and Jacobsen). They used a copper catalyst to activate the carbon reactant and then a hydrogen-bonding thiourea catalyst to set the product geometry with high selectivity. The reaction is compatible with a broad range of diazo ester and amine coupling partners.

*Science*, this issue p. 990; see also p. 948